

Kinetics and chemomechanical properties of the F_1 -ATPase molecular motor

Ming S. Liu, B. D. Todd, and Richard J. Sadus

Centre for Molecular Simulation, Swinburne University of Technology, P.O. Box 218, Hawthorn, Victoria 3122, Australia

(Received 3 September 2002; accepted 25 February 2003)

F_1 -ATPase hydrolyzes ATP into ADP and Pi and converts chemical energy into mechanical rotation with exceptionally high efficiency. This energy-transducing molecular motor increasingly attracts interest for its unique cellular functions and promising application in nanobiotechnology. To better understand the chemomechanics of rotation and loading dynamics of F_1 -ATPase, we propose a computational model based on enzyme kinetics and Langevin dynamics. We show that the torsional energy and stepwise rotation can be regulated by a series of near-equilibrium reactions when nucleotides bind or unbind, as well as characterized by an effective “ratchet” drag coefficient and a fitting chemomechanic coefficient. For the case of driving an actin filament, the theoretical load-rotation profile is analyzed and comparison with experimental data indicates reasonable agreement. The chemomechanics described in this work is of fundamental importance to all ATP-fueled motor proteins. © 2003 American Institute of Physics. [DOI: 10.1063/1.1568083]

I. INTRODUCTION

Molecular motors is a generic term for a group of proteins that generate cellular forces and motion by transducing chemical synthesis or hydrolysis energy into mechanical energy. In recent years, various motor proteins have been discovered and harnessed for the purpose of single molecule manipulation and nanobiotechnology.^{1,2} There are mechanically two broad types of motor proteins: linear motors and rotary motors. Linear motors may include myosin (dragging and rowing to contract muscle),^{3,4} kinesin (walking hand-over-hand along microtubules),^{4,5} and RNA polymerase or helicase (crawling to transcript gene codes),^{6,7} etc. Examples of rotary motors are flagellar (propelling bacteria through the viscous cell)^{8,9} and the enzyme ATP synthase (F_1F_o -ATPase, rotating while transducing energy from hydrolysis/synthesis of ATP molecules).^{10–17} All molecular motors are powered either by the hydrolysis or synthesis of nucleotides [e.g., adenosine triphosphate (ATP)], or by an electrochemical potential difference across the cytoplasmic membrane.

The F_1F_o -ATPase molecular motor possesses both types of driving forces. It synthesizes ATP from adenosine diphosphate (ADP) and inorganic phosphate (Pi) at the F_1 domain at the expense of protons from the F_o domain. Alternatively, when operating in the reverse, it hydrolyzes ATP into ADP and Pi at F_1 and releases energy. Coupling with the conversion of chemical energy, rotary mechanical torque is produced at F_1 domains in both cases.^{10,11,15,16} It is believed that proton transport and the synthesis of ATP by the holoenzyme are mechanically cooperative.^{11,17} The energy conversion mechanism in F_1F_o -ATPase represents a delicate blend of electrical-to-mechanical-to-chemical energy operations. Isolated F_1 is able to catalyze ATP hydrolysis but not net ATP synthesis. Thus individual F_1 -ATPase can also work independently as a motor, rotating the central “shaft” protein against surrounding subdomain proteins when ATP is hydro-

lyzed. Recently, F_1 -ATPase was explored as a possible means of propulsion for a nanomachine that is driven totally by biological power and has an exceptionally high chemomechanical coefficient.^{14,18–21}

To better understand the operating mechanism and rotary dynamics of F_1F_o -ATPase, various theoretical approaches have been used, such as microscopic modelling of the coupling of two driving-forces,^{22–25} and atomistic simulation using molecular dynamics methods.^{26,27} For example, the model of Wang and Oster^{22,23} provides a physically based answer to the rotational dynamics of F_1 -ATPase. It is a continuous model based on a system of coupled Fokker–Planck equations with an artificial energy landscape for the motor system. Their work gave arguably the best physical understanding of the dynamic mechanism of F_1 -ATPase to date. However, they ignored the biochemical details related to the ATP hydrolysis reactions. On the other hand, Panke *et al.*²⁴ determined a set of enzyme kinetic rates for ATPase, but gave only very rough results for the dynamical behavior of the motor system. In contrast to Wang and Oster^{22,23} and Panke *et al.*,²⁴ this work aims to establish a link from molecular-scale chemical hydrolysis reactions to microscale mechanical motion of the F_1 -ATPase molecular motor, and design a general simulation approach for the chemomechanics of such motor proteins. We propose a computational model based on enzyme kinetics and rotary Langevin dynamics, and regulate the energy transduction and stepwise rotation of F_1 -ATPase by a series of near-equilibrium reactions when nucleotides bind or unbind. To validate the model, we investigate the case of the F_1 -ATPase motor driving an actin filament, and analyze the theoretical load-rotation profile against some existing experimental results. The kinetics and chemomechanics described in this work is useful in furthering our understanding of ATP-fueled motor proteins.

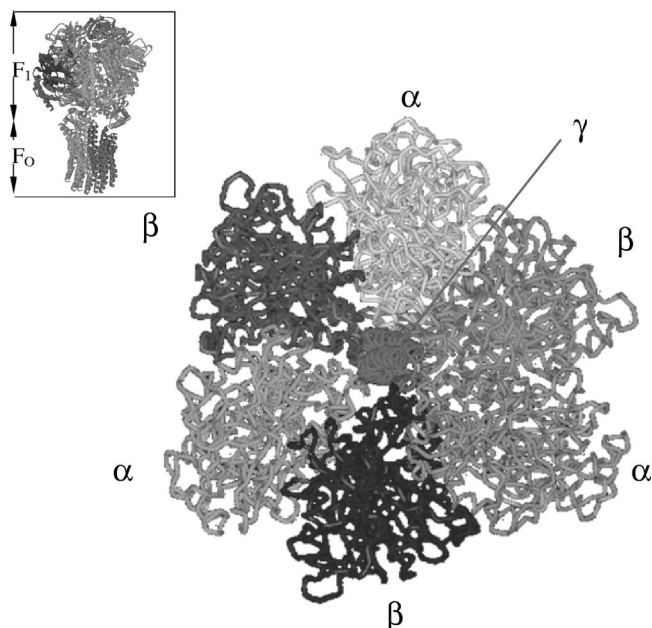


FIG. 1. A top-view of structures of the F_1 -ATPase molecular motor. The six large subunits ($\alpha\beta$)₃ form a hexamer that holds a spinning central shaft, subunits of γ ($\epsilon\delta$ are not marked). Inset is a side-view of F_1F_0 -ATP synthase of yeast mitochondria (ref: Protein Data Bank 1QO1).

II. THEORY OF THE KINETICS AND CHEMOMECHANICS OF THE F_1 -ATPase MOTOR

A. The mechanism of rotation of F_1F_0 -ATPase

Walker *et al.*^{15,17,28} revealed the stoichiometric structures of F_1F_0 -ATPase, as shown in Fig. 1 (a top-view of F_1 -ATPase): three α , three β , and one γ , δ , ϵ chain of proteins comprise the F_1 domain; one a , two b , 9 or 12 c chains of proteins form the F_0 domain. The F_1 and F_0 domains are linked by a central stalk composed of γ , δ , ϵ protein chains. Atomic-resolution structure studies suggest that the α_3 and β_3 subunits form a hexamer and the $\gamma\delta\epsilon$ subunits act as a shaft of rotation against the hexamer. For a typical F_1F_0 -ATPase molecular motor (such as yeast mitochondrial), the dimensions are about 12 nm wide and 22 nm high (the F_1 domain has a height of about 14 nm).¹⁵ It is found that three alternative sites on the hexagon formed by subunits ($\alpha\beta$)₃ are catalytic-active and responsible for the ATP hydrolysis/synthesis.^{10,11,17} Amongst the six subdomains (three α and three β subunits) in F_1 , three nucleotide sites of β subunits take the main responsibility for the nucleotide catalysis. These three sites either bind or unbind with ATP, ADP or inorganic P molecules or are empty, depending on their respective positions relative to the concave, neutral, or convex sides of the shaft γ subunit.

The rotation of F_1F_0 -ATPase was first reported by Duncan *et al.*²⁹ and Sabbert *et al.*,^{12,13} and the most compelling evidence was provided by the experiments of Noji *et al.*^{18–20} With a physiologically-cloned F_1 -ATPase motor, Noji *et al.*¹⁸ visibly demonstrated the ATP-driven rotary mechanism with an actin filament (typically 1–2 μm) attached as a fluorescent tag on one end of the γ subunit. They revealed that the rotation is three-stepped, with stepwise (120° per step) transitions between three symmetrically spaced angular

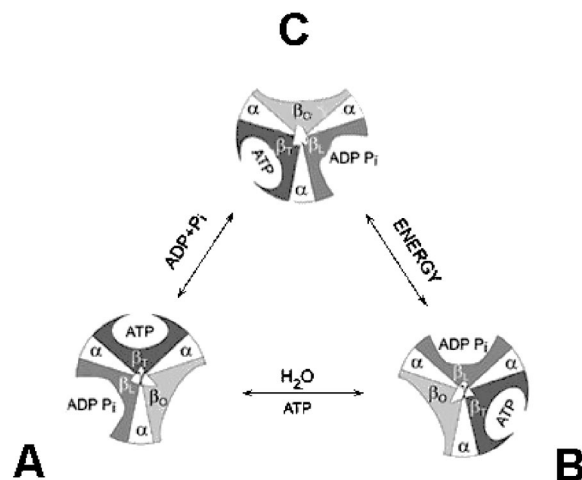


FIG. 2. Asymmetrical binding change mechanism of the hydrolysis in F_1 -ATPase proposed by Boyer (Refs. 10, 11, 30) (courtesy of The Nobel Foundation, 1997). Following counterclockwise, ABC represents a full cycle of F_1 -ATPase hydrolyzing ATP into ADP and Pi, meanwhile producing energy. Sections denoted ($\alpha\beta_T$), ($\alpha\beta_L$), and ($\alpha\beta_O$) refer to the conformational tight-binding, loose-binding, and open states of ($\alpha\beta$) pairs, respectively.

resting positions of γ relative to ($\alpha\beta$)₃. All these experiments, plus the structures revealed by Walker *et al.*,^{15,28} further verified the hydrolysis/synthesis mechanism proposed by Boyer.^{10,11,30} Currently the commonly accepted mechanism^{10,11,16,17} of F_1F_0 -ATPase features:

- (1) The catalytic nucleotide binding sites at three ($\alpha\beta$) pairs work in a cooperative way: while one site binds, the next one hydrolyzes ATP, and the third one intakes/releases the hydrolysis/synthesis products;
- (2) The sequential conformational changes in ($\alpha\beta$)₃ induce the rotary torque between the hexamer ($\alpha\beta$)₃ and the stalk γ - ϵ , and therefore makes the motor rotate stepwisely;
- (3) The F_0 -portion of F_1F_0 -ATPase probably also functions as a stepper motor when ion flow is pumped up the channel and the electrochemical energy is transferred from the F_0 portion into the F_1 portion, or vice versa.

In addition, the motor motions are bathed in constant Brownian fluctuations. Some works revealed that a structural “ratchet” mechanism (that can rectify Brownian motion) occurs at the central “shaft” ($\gamma\delta\epsilon$) subunits when rotating against surrounding subdomain proteins.⁴⁵

The mechanism, as illustrated in Fig. 2, suggests that three catalytic sites of ($\alpha\beta$)₃ exist in different conformation states at any given moment. Each possible conformation has a different bound nucleotide, thus the motor subunits are inherently asymmetric. On average, one site is bound with ATP, the second with ADP or ADP.Pi, and the third is enzymatically inactive, i.e., empty. The third site works for the exchange of substrates, i.e., ATP or ADP and Pi, with the environment. There is a cooperative coupling between the subunits via an indirect coupling mechanism that drives sequential structural conformations. This turns out to be a rotation of the γ subunit, which caused the further catalytic

binding changes at $(\alpha\beta)_3$ subunits. This requires interaction of three $(\alpha\beta)_3$ sites with high cooperativity.

B. Kinetic modeling of hydrolysis reactions in F_1 -ATPase

To model the kinetics and chemomechanics of the F_1 -ATPase molecular motor, we have two major tasks: one is to solve the enzyme kinetics of ATP hydrolysis and the other is to link this hydrolysis kinetics with chemomechanical transduction and mechanical rotation.

We assume that the multisite hydrolysis at three $(\alpha\beta)_3$ catalytic binding subunits are biochemically equal, and the ATP hydrolysis reaction is under steady-state conditions. Therefore, the cycles of hydrolysis reactions in F_1 -ATPase could be regarded as a threefold near-equilibrium process with the reaction sequence,



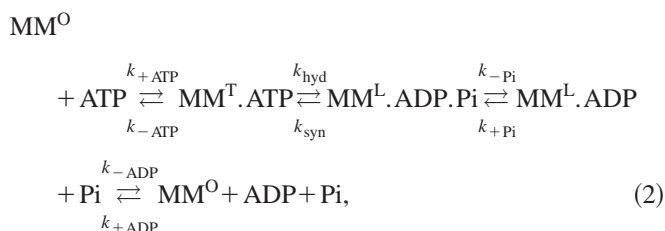
where MM^O refers to the bound-free state of the ATPase molecular motor. k_1 , k_{-1} , and k_2 , k_{-2} refer to the forward and backward reaction rate constants, respectively.

It is essential to consider the binding change mechanism and multisite cooperativity for ATP hydrolysis in F_1 -ATPase. Based on the Boyer mechanism,^{10,11,30} Fig. 2 presents a schematic diagram of the binding changes of F_1 -ATPase in a hydrolysis cycle of ATP. The catalysis multisites are noted as $\alpha\beta_{TB}$, $\alpha\beta_{LB}$, and $\alpha\beta_{open}$, where the open (O) site has a very low affinity for substrates of ATP, ADP or Pi and is catalytically inactive; a loosely bound (LB) site has loosely bound substrates and is catalytically inactive; and a tightly bound (TB) site has tightly bound substrates and is catalytically active. Three $(\alpha\beta)$ sites interact in a cooperative manner in each hydrolysis cycle as the central stalk γ subunit rotates relative to them sequentially. While one site binds, the next one hydrolyzes ATP, and the third one releases the hydrolysis products.

Accordingly, the following criteria are set up to model the catalytic hydrolysis in F_1 -ATPase:

- (1) At a given moment, each paired $\alpha\beta$ subunit is in an alternating conformational state, being noted as O, LB, and TB sites. In cycles of hydrolysis, three $(\alpha\beta)$ pairs synchronize to undergo conformational changes in a highly cooperative way.
- (2) The rotation of subunits $\gamma\delta\epsilon$ relative to the $(\alpha\beta)_3$ hexamer, via cooperative interactions among the catalytic sites, drives each binding site to repeat from $O \rightarrow TB \rightarrow LB \rightarrow O$. Coupled with the $TB \rightarrow LB$ transition, ATP is hydrolyzed into ADP and Pi, or reversibly for synthesis. Simultaneously with ATPase completing its catalytic cycle in a threefold repetition, $\gamma\delta\epsilon$ subunits rotate stepwisely.
- (3) There is a competition of chemical reaction equilibrium between ATP hydrolysis and ATP synthesis. For F_1 -ATPase under stand-alone conditions, the overall reaction should favor ATP hydrolysis.
- (4) Chemomechanically, F_1 -ATPase converts the chemical energy from hydrolysis into continuous rotational energy with a certain efficiency.

To take into account that the unbinding and release of ADP and Pi are in the sequence of Pi first followed by ADP, a complete enzymatic cycle at each $(\alpha\beta)$ pair in F_1 -ATPase would follow the pathway of,^{16,17}



k_{ATP} , k_{-ATP} refer to the rate constants of association and dissociation of ATP molecules to the motor (or namely, the rate of binding to or unbinding from enzymatic-active sites of the motor protein). The same definition applies for k_{ADP} , k_{-ADP} and k_{Pi} , k_{-Pi} . k_{hyd} , k_{syn} refers to the binding change rate constants of ATP hydrolysis and synthesis.

Under the steady-state assumption, we interpret the whole cycle of Eq. (2) by a series of fast equilibrium reactions,

$$\begin{aligned} P_O + P_{ATP} + P_{ADP \cdot Pi} + P_{ADP} &= 1, \\ k_{ATP} \cdot [ATP] \cdot P_O + k_{syn} \cdot P_{ADP \cdot Pi} - (k_{hyd} + k_{-ATP}) \cdot P_{ATP} &= 0, \\ k_{hyd} \cdot P_{ATP} + k_{Pi} \cdot [Pi] \cdot P_{ADP} - (k_{syn} + k_{-Pi}) \cdot P_{ADP \cdot Pi} &= 0, \\ k_{-Pi} \cdot P_{ADP \cdot Pi} + k_{ADP} \cdot [ADP] \cdot P_{open} - (k_{Pi} \cdot [Pi] + k_{-ADP}) \cdot P_{ADP} &= 0, \\ k_{-ATP} \cdot P_{ATP} + k_{-ADP} \cdot P_{ADP} - (k_{ATP} \cdot [ATP] + k_{ADP} \cdot [ADP]) \cdot P_O &= 0, \end{aligned} \quad (3)$$

where $[ATP]$, $[ADP]$, and $[Pi]$ are the concentrations of ATP, ADP, and Pi, respectively. P_O , P_{ATP} , $P_{ADP \cdot Pi}$, and P_{ADP} are the probability of the states when different pairs of $(\alpha\beta)_3$ are either empty or occupied by ATP, ADP.Pi or ADP molecules,

respectively (as illustrated in Fig. 2 and described in the above criteria). Here we assume that the F_1 -ATPase motor is bathed in water and ATP, ADP, and Pi molecules are fully dissolved in solution. Equation (3) is a translation of Eq. (2)

in steady-state cycles, which is justified by the fact that the rotational motion and the chemical reaction steps are repeatedly coupled.

From Eq. (2), the overall reaction rate of catalytic hydrolysis can be calculated by

$$R = k_{\text{hyd}}P_{\text{ATP}} - k_{\text{syn}}P_{\text{ADP}\cdot\text{Pi}} \quad (4)$$

Substituting Eq. (3) into Eq. (4) gives the overall hydrolysis reaction rate of F₁-ATPase as,

$$R = (-k_{-\text{ATP}}k_{\text{syn}}k_{\text{ADP}}[\text{ADP}]k_{\text{Pi}}[\text{Pi}] + k_{-\text{ADP}k_{-\text{Pi}}k_{\text{hyd}}k_{\text{ATP}}[\text{ATP}]) / (k_{-\text{ADP}k_{-\text{Pi}}k_{\text{hyd}}} + (k_{\text{hyd}}k_{-\text{Pi}} + k_{-\text{ATP}k_{-\text{Pi}} + k_{-\text{ATP}k_{\text{syn}}} + (k_{-\text{ATP}} + k_{\text{syn}} + k_{\text{ADP}})k_{\text{Pi}}[\text{Pi}])k_{\text{ADP}}[\text{ADP}] + k_{\text{hyd}}(k_{-\text{ADP}} + k_{-\text{Pi}} + k_{\text{Pi}}[\text{Pi}])k_{\text{ATP}}[\text{ATP}] + (k_{-\text{ADP}k_{-\text{Pi}} + k_{-\text{ADP}k_{\text{syn}} + k_{\text{syn}}k_{\text{Pi}}[\text{Pi}])k_{-\text{ATP}} + k_{\text{ATP}}[\text{ATP}])). \quad (5)$$

Given a physiological condition, such as the concentrations of ATP, ADP, and Pi, the steady kinetics of F₁-ATPase will obey the above equations and the overall hydrolysis rate is computable via Eq. (5). It should be noted that the same rate constants are used for the different [ATP], [ADP], and [Pi] conditions.

In the limit of small product concentration, synthesis can be neglected and the overall reaction rate of Eq. (5) becomes,

$$R = k_{-\text{ADP}k_{-\text{Pi}}k_{\text{hyd}}k_{\text{ATP}}[\text{ATP}] / (k_{-\text{ADP}k_{-\text{Pi}}k_{\text{hyd}}} + k_{-\text{ATP}k_{-\text{ADP}k_{-\text{Pi}} + k_{-\text{ATP}k_{-\text{ADP}k_{\text{syn}}} + (k_{\text{hyd}}k_{-\text{ADP}} + k_{\text{hyd}}k_{-\text{Pi}} + k_{-\text{ADP}k_{-\text{Pi}} + k_{-\text{ADP}k_{\text{syn}}})k_{\text{ATP}}[\text{ATP}])). \quad (6)$$

This is the format of so-called Michaelis–Menten kinetics,³¹ $R = R_{\text{max}}[\text{ATP}] / (K_m + [\text{ATP}])$, with now a Michaelis constant of

$$K_m = \frac{k_{-\text{ADP}k_{-\text{Pi}}k_{\text{hyd}} + k_{-\text{ATP}k_{-\text{ADP}k_{-\text{Pi}} + k_{-\text{ATP}k_{-\text{ADP}k_{\text{syn}}}}}{(k_{\text{hyd}}k_{-\text{ADP}} + k_{\text{hyd}}k_{-\text{Pi}} + k_{-\text{ADP}k_{-\text{Pi}} + k_{-\text{ADP}k_{\text{syn}}})k_{\text{ATP}}}$$

moles per liter.

C. Chemomechanics of the rotary motion of F₁-ATPase

How is the chemical energy from ATP hydrolysis converted into rotational motion in the F₁-ATPase motor? The ultimate answer to this question depends on whether the chemical potential energy landscape is precisely known. While this is not known to date, a good approximation is important. To reveal the chemomechanics and rotary dynamic behavior of F₁-ATPase, a system of the F₁-ATPase motor driving a load could be treated as an ensemble of polymeric proteins rotating while floating in a solvent bath. The energetics of such a system basically consists of catalytic hydrolysis, mechanical rotation, external forces, and constant Brownian fluctuation of the whole system in a thermal bath. In such a case, one could model it by rotary Langevin dynamics.

A master equation of Langevin dynamics of a rotating F₁-ATPase motor can be written as,^{22,23,32}

$$\omega = \frac{d\theta}{dt} \hat{\theta},$$

$$\frac{d\mathbf{L}}{dt} = \tau_{mm} + \tau_{\text{ext}} - \zeta \omega + \tau_B(t), \quad (7)$$

where ω is the angular velocity and θ the mechanical position (with rotation only occurring in the x–y plane), $\mathbf{L} = \mathbf{I}\omega$ is the angular momentum of the system, and \mathbf{I} is the moment of inertia tensor; τ_{mm} is the torque generated directly from the hydrolysis reactions at corresponding functional subunits of the F₁ motor, $\tau_{mm} = -[\partial U(\theta)/\partial \theta]$, and $U(\theta)$ is the corresponding chemical potential energy at position θ of the molecular motor. It is expected that the molecular motor will switch between a series of $U(\theta)$ when it rotates and undergoes continuous conformational changes; τ_{ext} is the torque on a load applied by an external force (if any); $\zeta \omega$ is the torque via frictional drag in a viscous medium, with ζ the drag coefficient of the load against the media; τ_B is the Brownian motion term due to thermal fluctuation-dissipation of the acting subunits of F₁-ATPase and its loading.

Given that the very fast Langevin relaxation time, I/ζ , is approximately 2×10^{-12} s for the case of F₁ driving an actin filament, a steady state approximation implies that the moment of inertia is constant and the angular momentum should be conserved, i.e.,

$$\left\langle \frac{d\mathbf{L}}{dt} \right\rangle_t \equiv 0, \left\langle \frac{d\mathbf{L}}{dt} \right\rangle_\theta \equiv \zeta_r \bar{\omega},$$

$$\langle \tau_B(t) \rangle \equiv 0, \langle \tau_B(0) \tau_B(t) \rangle \equiv 2k_B T \zeta \delta(t), \quad (8)$$

where $\delta(t)$ is the Dirac δ -function and the fluctuating torque is represented by Gaussian white noise. To account for the “ratchet” mechanism occurring at central stalk subunits when they rotate against surrounding subdomains, we assume that the average angular momentum at any given time is in effect a constant drag torque, $\zeta_r \bar{\omega}$. Here a fitting constant, ζ_r , is introduced as the effective “ratchet” drag coefficient. This “ratchet” Brownian mechanism at the rotating subunits of the motor will keep it spinning unidirectionally (for detailed discussions, see Sec. III C).

If the chemical potential energy landscape $U(\theta)$ and the binding sites occupation vs the position are precisely known, the rotary dynamics of the F₁-ATPase motor (when driving a load) can be precisely described by Eqs. (7) and (8). However, an approximation has to be made to implement the Langevin dynamics, given that no such landscape has been determined for any motor proteins to date. For example, Wang and Oster^{22,23} adopted a hypothetical potential and statistically averaged a collection of probability densities via the equations of continuity. For simplicity we assume that all the chemical energy of hydrolysis is convertible into mechanical energy (via conformational changes of the $\alpha_3\beta_3\gamma\delta\epsilon$ complex), and finally turned into workable torque between the $\gamma\delta\epsilon$ and $(\alpha\beta)_3$ subunits.

When an F₁-ATPase motor works steadily (such as when it drives an actin filament), it was demonstrated that a 3

TABLE I. The kinetic parameters for simulation of the F₁-ATPase molecular motor.

Rate constants ^a of substrate association and dissociation (indicated by -):	$k_{\text{ATP}}=2.08\times 10^6 \text{ M}^{-1} \text{ s}^{-1}$ $k_{\text{ADP}}=8.90\times 10^6 \text{ M}^{-1} \text{ s}^{-1}$ $k_{\text{Pi}}=8.10\times 10^5 \text{ M}^{-1} \text{ s}^{-1}$	$k_{-\text{ATP}}=2.70\times 10^2 \text{ s}^{-1}$ $k_{-\text{ADP}}=4.90\times 10^2 \text{ s}^{-1}$ $k_{-\text{Pi}}=2.03\times 10^3 \text{ s}^{-1}$
Rate constants ^a of binding changes of ATP hydrolysis and synthesis	$k_{\text{hyd}}=4.5\times 10^5 \text{ s}^{-1}$ $k_{\text{syn}}=1.15\times 10^{-3} \text{ s}^{-1}$	
Effective “ratchet” drag coefficient	$\sim 1.07 \text{ pN nm s}$	

^aFrom Panke and Rumberg, Ref. 24.

$\times 120^\circ$ stepwise rotation is accomplished with the hydrolysis of ATP molecules.^{18,19,21} Therefore we have, on average, $\Delta U(\theta) = R\Delta G_{\text{hyd}}\Delta t$, which leads to

$$\left\langle \frac{\partial U(\theta)}{\partial \theta} \right\rangle = \frac{\eta R \Delta G_{\text{hyd}}}{\bar{\omega}}. \quad (9)$$

Here we introduce η as the chemomechanical coefficient, which indicates the efficiency of the F₁-ATPase motor in converting ATP hydrolysis energy into rotary torque. The perfect motor would possess η of 100%. For a practical molecular motor, η is less than 100% due to the fact that the motor is not a steady chemomechanical equilibrium system and it will have some energy dissipation, such as heat dissipation. As discussed previously, R is the overall ATP hydrolysis rate of F₁-ATPase [see Eqs. (5) and (6)]. In Eq. (9), the chemical energy released from ATP hydrolysis reactions is,³¹

$$\Delta G_{\text{hyd}} = G_o + k_B T \ln \frac{[\text{ADP}][\text{Pi}]}{[\text{ATP}]}, \quad (10)$$

with $G_o \approx -50.74 \text{ pN nm}$ for the free energy released from the hydrolysis of a single ATP molecule at $\text{pH}=7$ at 25°C .

Equation (9) actually reveals the energy transduction nature in the F₁-ATPase motor, which indicates how the enzyme kinetic entities are exerted into mechanical torques. Together, Eqs. (7)–(9) provide a full description of the chemomechanical properties of the F₁-ATPase motor.

D. When F₁-ATPase drives an actin filament

F₁-ATPase has been developed as a unique nanomachine to drive a load, most successfully to drive an actin filament, with an exceptionally high thermodynamic coefficient.^{14,18–21} To validate the model developed through Secs. II A to II C, we now consider the case of a rotating F₁-ATPase motor driving an actin filament. For the sake of simplicity, we coarse-grain the mechanical difference when the motor switches between various chemical states during rotation (in particular when ATP, ADP molecules bind or unbind to the motor), and assume F₁-ATPase is a steady motor and there is no external torque. The actual inertia term of the load, such as an actin filament, can be omitted as it is much smaller than the drag torque. Therefore using Eqs. (9) and (8) in conjunction with the average of Eq. (7), we have

$$\bar{\omega} \approx \frac{1}{(\zeta + \zeta_r)} \left[\left\langle \frac{\partial U(\theta)}{\partial \theta} \right\rangle + \bar{\tau}_B \right], \quad (11)$$

where the time-averaged Brownian torque, $\bar{\tau}_B$, can be derived from $\sqrt{\langle \bar{\tau}_B^2 \rangle} \approx \sqrt{2k_B T \zeta / 3 \Delta t}$ with Δt the perturbing time of the Brownian fluctuation.³³ ζ_r is the fitting parameter. Physically it is the effective “ratchet” drag exerted by the $\alpha_3\beta_3\gamma\delta\varepsilon$ subunits, which we introduced in Eq. (8) and will discuss later. In the case of F₁-ATPase driving a load of an actin filament, the drag coefficient may be expressed as³⁴

$$\zeta = \frac{4\pi}{3} \zeta_o l^3 \left/ \left[\ln \frac{l}{2r} - 0.447 \right] \right. . \quad (12)$$

Here, $\zeta_o \sim 1 \times 10^{-3} \text{ N m}^{-2} \text{ s}$ is the viscosity of the media, l and r ($\sim 5 \text{ nm}$) are the length and the radius of the filament, respectively.^{18–20}

Substituting Eqs. (5), (9), (10), and (12) into Eq. (11) allows us to determine the chemomechanical properties of the F₁-ATPase molecular motor when it drives an actin filament. For example, the rotational rate of the F₁ motor as a function of nucleotide concentrations and actin length can be determined.

III. RESULTS AND DISCUSSIONS

A. Overall hydrolysis reaction rate

From Eqs. (4) and (5), we determine the overall hydrolysis reaction rate of F₁-ATPase at certain given kinetic conditions, e.g., the concentrations of binding nucleotides ATP, ADP or Pi. The rate constants of association/dissociation and the reaction rate constants of hydrolysis/synthesis can be obtained by conventional enzyme kinetics experiments. However, it should be noted these rate constants are far from being consistent and they change from experiment to experiment for different F₁F_o-ATPase enzymes.

Table I gives a full set of rate constants of chloroplasts F₁F_o-ATPase enzyme measured by Panke *et al.*²⁴ Assuming the rate constants of F₁-ATPase from Table I, Fig. 3 shows an overall hydrolysis reaction rate changing versus [ATP] without inhibition of ADP or Pi. The calculation (solid line in Fig. 3) is compared with experimental data of the *Bacillus PS3* F₁-ATPase motor^{19,20} (diamonds in Fig. 3). The overall agreement between calculation and experiment is reasonable. The difference can be partly attributed to the fact that the motor experiments used different enzyme proteins (*Bacillus PS3*) from our computation (chloroplasts), as the complete enzyme kinetic data of *Bacillus PS3* is not currently avail-

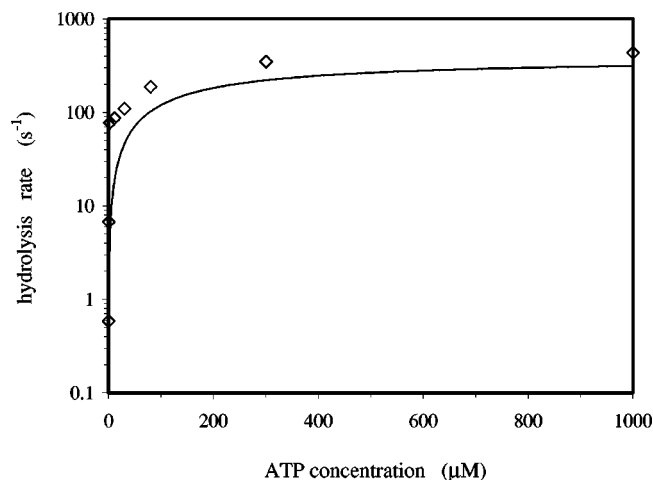


FIG. 3. Overall hydrolysis reaction rate of F_1 -ATPase vs ATP concentration, [ATP]. The diamonds refer to experimental data from Yasuda *et al.* (Refs. 19 and 20).

able. The slower rate for lower [ATP] is due to the lower turnover of ATP binding and hydrolysis. With higher [ATP], the steady-state overall hydrolysis reaction rate, R , of F_1 -ATPase increases rapidly and becomes saturated with ATP above ~ 300 s $^{-1}$ (for comparison, R at saturation will be only about 10 s $^{-1}$ if taking the set of rate constants of Cross *et al.*³⁵ which measured a unisite hydrolysis of mitochondria F_1 -ATPase). Fitting our theoretical results with the Michaelis–Menten equation, $R = R_{\max}[\text{ATP}]/(K_m + [\text{ATP}])$, we determined the Michaelis constant to be $K_m \sim 181$ μM for chloroplasts F_1F_0 -ATPase. This theoretical K_m value is comparable to the experimental value³⁶ of mitochondrial F_1 -ATPase ($K_m \sim 130$ μM) but is larger than the experimental value^{19,20} of *Bacillus PS3* F_1 -ATPase ($K_m \sim 15$ μM). We also found that the overall hydrolysis reaction rate R could approach zero when choosing certain sets of values of [ATP], [ADP], [Pi] and rate constants. In those cases, F_1 -ATPase no longer undergoes hydrolysis.

We developed our kinetics model on the basis of Boyer's bisite catalysis mechanism, with three ($\alpha\beta$) sites involved in a cooperative manner. However, the binding change concept and catalytic cooperativity are still unclear. Nakamoto *et al.*³⁷ reviewed the catalysis of F_1F_0 -ATPase and found that biochemically it can undergo both unisite catalysis and multisite catalysis. When [ATP] is in substoichiometric quantity, it binds to the first site with very high affinity. As this ATP is hydrolyzed to ADP+Pi, the products are released slowly (with the rate constant $k < 10^{-3}$ s $^{-1}$). Instead, reversible hydrolysis/synthesis occurs with an equilibrium constant close to 1, which leads to unisite catalysis. Multisite catalysis occurs when [ATP] is high enough to bind to the next site. The positive cooperative interactions between the binding sites is manifest by lower affinity binding, which promotes the competitive chase of ATP and ADP+Pi bound in the first site.³⁷ Senior *et al.*^{38–40} also investigated the catalysis of isolated F_1 -ATPase of *E. Coli*. The catalysis-related rotation of the $\gamma\delta\epsilon$ subunits relative to three $\alpha\beta$ subunits of the isolated F_1 takes place as in F_1F_0 , and identical conformation changes of γ and ϵ occurred in F_1 and in F_1F_0 . At low ATP

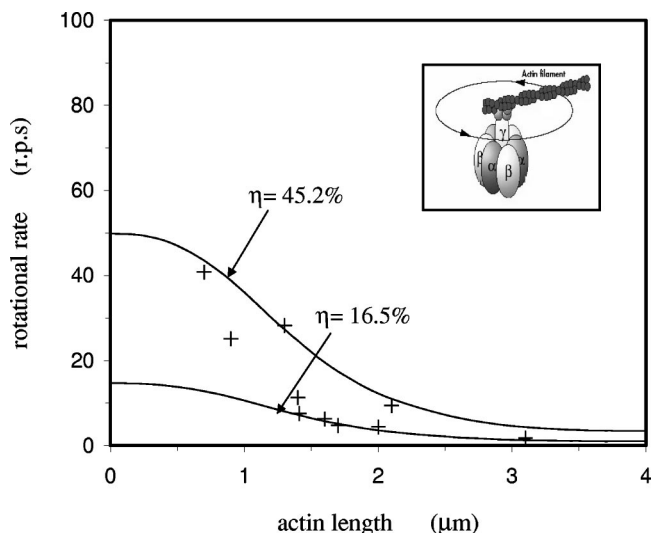


FIG. 4. The rotational rate of F_1 -ATPase as it drives an actin filament (inset diagram shows such a scenario). The crosses are from experimental measurements, (Ref. 19) and the two solid lines indicate that F_1 -ATPase works at different chemomechanical coefficients with an effective “ratchet” drag coefficient of 1.07 pN nm s. [ATP], [ADP], and [Pi] are set as 2 mM, 10 μM , and 10 mM, respectively.

concentration (< 1 μM), when primarily the high affinity site was occupied, the ratio of enzyme-bound ADP to ATP was about 0.5 (which reflects the reaction equilibrium constant in unisite catalysis). At high ATP concentration [≥ 1 μM , e.g., in the range of (100 μM –mM)], it is a trisite hydrolysis mechanism and all three catalysis sites are occupied and filled with ATP or ADP, and the probability of an empty site is rare.

In F_1 -ATPase, the effect of the binding sites of either unisite, bisite or trisite occupation on the hydrolysis reaction is not fully understood. This certainly affects the configuration of our model. As discussed elsewhere,^{17,40} there is still disagreement about the binding change mechanism and pathways of hydrolysis reactions. The disagreement will hopefully be resolved when more comprehensive experimental measurements are made. In our present work, we follow the bisite hydrolysis model and simply take the rate constants as fixed.

B. The rotary motion under kinetic and loading conditions

By substitution of Eqs. (8), (9), and (12) into Eq. (11), we could determine the chemomechanical properties of the F_1 -ATPase molecular motor when it drives an actin filament. The dependence of rotation rate upon the length of loading actin is plotted in Fig. 4 (solid lines). The rotation rate is in the units of radians per second (rad s $^{-1}$). In order to compare with experiments,^{18–21} we used [ATP], [ADP], and [Pi] of 2 mM, 10 μM , and 10 mM, respectively. The crosses in Fig. 4 are from experimental measurements,¹⁹ and the two solid lines indicate that the F_1 -ATPase motor works at chemomechanical coefficients within the range $16.5\% \leq \eta \leq 45.2\%$. The effective “ratchet” drag coefficient, which is 1.07 pN nm s in this case, is calculated to ensure the rotational rates' convergence at zero length and to comprise the

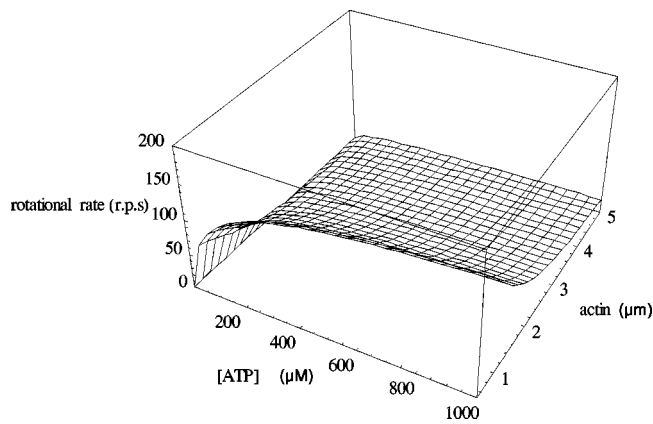


FIG. 5. The rotational rate of F₁-ATPase vs ATP concentration and the length of actin filament. The rate is in units of radians per second. [ADP] and [Pi] are set to 10 μM and 0.1 mM, respectively.

top and bottom range of scattered experimental data. This value is found to be close to the drag coefficient of driving a 1-μm actin filament at one end.

Yasuda *et al.*^{16,18–20} claimed that the F₁-ATPase-actin motor system would have a thermodynamic coefficient of about 100%. Soong *et al.*²¹ also report that a F₁-ATPase-nanopropeller system may have a thermodynamic coefficient of ~80%. However, as seen in Fig. 4, the fit of our model to the experimental data indicates that this may not be the case. The experimental data are widely scattered, and our theoretical rotational rates show that the motor system works with chemomechanical coefficients in the range of $\eta = 16.5\%$ to $\eta = 45.2\%$. Even considering the possibility of inhibitions of ADP or Pi, given the overall hydrolysis reaction rate as shown in Fig. 3 (both experimentally and theoretically), we could not reproduce the rotational rate (shown as the crosses in Fig. 4) with a coefficient of 100% or 80%. However, as recently proposed by Wang and Oster,⁴¹ the thermodynamic energy conversion efficiency and the chemomechanical energy transduction efficiency for molecular motors may need clarification. In addition, the extent to which the temperature variation and particularly the constant Brownian fluctuations contribute to the motions of the motor system is unknown either at molecular or micro scales.

To avoid the above difficulty, and for the purpose of understanding the mechanism, we now assume a 100% chemomechanical coefficient for the ideal F₁-ATPase motor

system. Using the rate constants of F₁-ATPase given in Table I, Fig. 5 and Fig. 6(a) show the rotational rates of an ideal F₁-ATPase motor (without external perturbations) against the length of actin filament at different ATP concentration, where [ADP] and [Pi] are set to meet physiological experimental conditions.^{18–20} The slower rate of rotation is expected for longer actin filaments due to higher friction at fixed [ATP]. Figure 3 indicates that the saturation rate of ATP hydrolysis reaction in the absence of load can reach about 300 s⁻¹. This implies that the maximal rotational rate of a load-free and inhibition-free motor could be about 600 rad s⁻¹. Our simulations show that the saturation rotation rate of F₁-ATPase, without actin load but with ADP and Pi inhibitions, will be about 180 rad s⁻¹. It becomes about 150 rad s⁻¹ with actin length of 1 μm or about 30 rad s⁻¹ with actin of 4 μm with [ATP] saturation. In this case, the torque exerted by the F₁-ATPase motor on an actin filament of 1 μm is calculated to be about ~150 pN nm. The chemomechanical properties (the rotation-actin length profiles) depicted here are both qualitatively and quantitatively consistent with experimental observation.^{18–20}

C. The “ratchet” mechanism and Brownian fluctuation

A ratchet, in biophysics, is a mechanism that can utilize random thermal fluctuations to generate a unidirectional drive in cellular processes. In the F₁-ATPase motor, constant Brownian motion of protein chains, as well as the load (such as an actin filament), will affect its enzymatic reactions and conformational dynamics, and therefore induce a mechanical contribution to the force of the whole system. Brownian fluctuation may play significant roles at very short time intervals and highly localized spaces, in particular within the nonequilibrium areas where the ATP hydrolysis reaction occurs and there is strong interaction between the binding molecules and surrounding protein. In molecular motors, such Brownian motion is no longer simply the universal random walk but rather a biased motion—the so-called “ratchet” Brownian motion.^{23,33,42–44} The Brownian force from such a “ratchet” mechanism will produce a kind of driving diffusion on acting domains of the motor proteins and make them move unidirectionally at large time and space scales. For the F₁-ATPase molecular motor, it has been argued²⁸ that torque applied to the central shaft rotates its convex surface toward the site

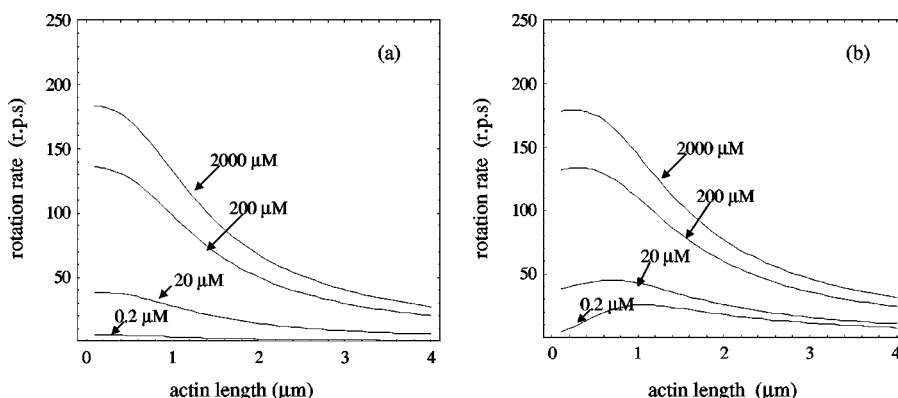


FIG. 6. The rotational rate of F₁-ATPase vs the length of the actin filament when the average effect of external Brownian fluctuation is not considered (a) or considered (b). Arrows indicate different ATP concentrations ([ADP] and [Pi] are set consistently as 10 μM and 0.1 mM).

filled with ATP and pushes the lower level of the respective β subunit outwards. This conformational change opens the ATP-binding site to expel the newly synthesized but firmly bound ATP into the bulk and is the major energy-requiring step of ATP synthesis.^{17,28} It was initially believed that a “ratchet” mechanism exists at the central “shaft” ($\gamma\delta\epsilon$) subunits when rotating against surrounding subdomain proteins. It has now been demonstrated experimentally⁴⁵ that the large conformational changes of subunits $\gamma\epsilon$, in particular ϵ , do provide a “ratchet” mechanism to regulate the unidirectional rotation of F₁F_o-ATPase.

In the F₁-ATPase motor, Brownian fluctuations are so rapid that they can be considered to be approximately at equilibrium on the time scale of measurement. Nevertheless, it remains unknown what the effect of Brownian motion is on the catalysis reactions, or how the fluctuation of loading molecules is transduced interactively to the fluctuation of the acting subdomains. It is known that the F₁-ATPase motor may have a force term generated by the “ratchet” Brownian fluctuation.²³ In this work, we introduce an effective drag constant, ζ_r , to account for the “ratchet” force harnessed by the motor itself from constant Brownian fluctuations. Our approach is to split the Brownian contribution into two parts: one is the effective drag force at $\gamma\epsilon$ subunits where the “ratchet” mechanism takes place, and the remaining contribution is a disturbing term at the load. In Eqs. (8) and (11), the parameter ζ_r accounts for the former component and $\bar{\tau}_B$ refers to the Brownian term from the loading actin filament and external perturbation. This treatment is justified as we attribute the internal Brownian fluctuation into the fitting parameter of ζ_r without knowing the exact potential landscape [i.e., $U(\theta)$] in F₁-ATPase. This process thus averages the stochastic nature of internal fluctuations and accumulates the overall force from Brownian motions at the motor proteins.

Our model shows that the value of ζ_r is fit at about 1.07 pN nm s. This value is close to the drag coefficient of driving a 1- μm actin filament at one end. It is of interest to note that Wang and Oster's simulations²³ with the stochastic Smoluchowski equations were applied with a diffusion constant, D , of 4.0 rad² s⁻¹, which also corresponds to the diffusion constant of a 1- μm actin filament rotating around one end. For $\bar{\tau}_B$ in Eq. (11), we assume that the Brownian average from a loading actin filament (as a part of the motor system) is zero, and the external perturbation can be calculated via $\sqrt{\langle \bar{\tau}_B^2 \rangle} = \sqrt{2k_B T \zeta / 3 \Delta t}$.³³ Δt is the perturbing time of the external disruptions. For stand-alone F₁-ATP synthase, the enzyme carries out rapid and uniaxial Brownian rotation with a rotational relaxation time about tens of milliseconds (ms).^{12,13} When F₁-ATPase drives an actin filament, Δt is mainly induced from passive imaging snapping and is in the range from ~ 1 ms to ~ 1 s.^{14,18–21} We used a value of 10 ms for our simulation, which is also a typical period of rotation of a load-free F₁-ATPase motor.¹⁹ Figure 6 shows the rotation rate versus the length of actin filament without [Fig. 6(a)] or with [Fig. 6(b)] the Brownian contribution of external perturbations. The Brownian fluctuations do slightly affect the overall chemomechanical behavior, especially when the load is close to zero. The small bumps in Fig. 6(b) imply that external perturbations may speed up the rotation of the system.

IV. CONCLUSIONS

We have successfully built a model describing the chemomechanics in the F₁-ATPase molecular motor. Based on enzyme kinetics and rotary Langevin dynamics, a link is established between molecular-scale chemical hydrolysis reactions and microscale mechanical motion of the F₁-ATPase motor. In a computational approach of such a link, we regulate the energy transduction and stepwise rotation by a series of near-equilibrium reactions when nucleotides bind or unbind. For the case of the F₁-ATPase motor driving an actin filament, our theoretical load-rotation profile reproduces the experimental results with reasonable accuracy. The kinetics and chemomechanics described here will hopefully lead to more fundamental understanding of ATP-fueled motor proteins.

ACKNOWLEDGMENTS

The authors thank the Victorian Partnership for Advanced Computing for partial support to M.S.L. and generous allocation of computing resources. We thank Dr. Matthew Downton for helpful discussions.

¹W. Junge, Proc. Natl. Acad. Sci. U.S.A. **96**, 4735 (1999).

²T. R. Strick, J-F. Allemand, V. Croquette, and D. Bensimon, Phys. Today **54**, 46 (2001).

³J. A. Spudich, Nature Rev. **2**, 387 (2001).

⁴R. D. Vale and R. A. Milligan, Science **288**, 88 (2000).

⁵M. J. Schnitzer, K. Visscher, and S. M. Block, Nat. Cell Biol. **2**, 718 (2000).

⁶M. D. Wang, M. J. Schnitzer, H. Yin, R. Landick, J. Gelles, and S. M. Block, Science **292**, 902 (1998).

⁷J. Gelles and R. Landick, Cell **93**, 13 (1998).

⁸S. Berry and H. C. Berg, Biophys. J. **76**, 580 (1999).

⁹D. R. Thomas, D. G. Morgan, and D. J. DeRosier, Proc. Natl. Acad. Sci. U.S.A. **96**, 10134 (1999).

¹⁰P. D. Boyer, Annu. Rev. Biochem. **66**, 717 (1997).

¹¹P. D. Boyer, Nature (London) **402**, 247 (1999).

¹²D. Sabbert, S. Engelbrecht, and W. Junge, Nature (London) **381**, 623 (1996).

¹³D. Sabbert, S. Engelbrecht, and W. Junge, Proc. Natl. Acad. Sci. U.S.A. **94**, 4401 (1997).

¹⁴O. Pänke, D. A. Cherepanov, K. Gumbiowski, S. Engelbrecht, and W. Junge, Biophys. J. **81**, 1220 (2001).

¹⁵D. Stock, A. G. W. Leslie, and J. E. Walker, Science **286**, 1700 (1999).

¹⁶K. Kinosita, Jr., R. Yasuda, H. Noji, and K. Adachi, Philos. Trans. R. Soc. London, Ser. B **355**, 473 (2000).

¹⁷R. Ian Menz, J. E. Walker, and A. G. W. Leslie, Cell **106**, 331 (2001).

¹⁸H. Noji, R. Yasuda, M. Yoshida, and K. Kinosita, Jr., Nature (London) **386**, 299 (1997).

¹⁹R. Yasuda, H. Noji, K. Kinosita, and M. Yoshida, Cell **93**, 1117 (1998).

²⁰R. Yasuda, H. Noji, M. Yoshida, K. Kinosita, and H. Itoh, Nature (London) **410**, 898 (2001).

²¹R. K. Soong, G. D. Bachand, H. P. Neves, A. G. Olkhovets, H. G. Craighead, and C. D. Montemagno, Science **290**, 1555 (2000).

²²H. Y. Wang and G. Oster, Nature (London) **396**, 279 (1998).

²³H. Y. Wang and G. Oster, Appl. Phys. A: Mater. Sci. Process. **75**, 315 (2002).

²⁴O. Panke and B. Rumberg, Biochim. Biophys. Acta **1412**, 118 (1999).

²⁵D. A. Cherepanov and W. Junge, Biophys. J. **81**, 1234 (2001).

²⁶R. A. Bockmann and H. Grubmüller, Nat. Struct. Biol. **9**, 198 (2002).

²⁷J. P. Ma, T. C. Flynn, Q. Cui, A. G. W. Leslie, J. E. Walker, and M. Karplus, Structure (London) **10**, 921 (2002).

²⁸J. P. Abrahams, A. G. W. Leslie, R. Lutter, and J. E. Walker, Nature (London) **370**, 621 (1994).

²⁹T. M. Duncan, V. V. Bulygin, Y. Zhou, M. L. Hutcheon, and R. L. Cross, Proc. Natl. Acad. Sci. U.S.A. **92**, 10964 (1995).

- ³⁰P. D. Boyer, in *Dynamics of Energy Transducing Membranes*, edited by L. Emster, R. Estabrook, and E. C. Slater (Elsevier, Amsterdam, 1974), pp. 289–301.
- ³¹A. Fersht, *Structure and Mechanism in Protein Science: A Guide to Enzyme Catalysis and Protein Folding* (Freeman, New York, 1999), Chap. 3.
- ³²M. Doi and S. F. Edwards, *The Theory of Polymer Dynamics* (Oxford University Press, Oxford, 1986).
- ³³R. F. Fox and M. H. Choi, *Phys. Rev. E* **63**, 051901 (2001).
- ³⁴A. J. Hunt, F. Gittes, and J. Howard, *Biophys. J.* **67**, 766 (1994).
- ³⁵D. Cunningham and R. L. Cross, *J. Biol. Chem.* **263**, 850 (1988).
- ³⁶Y. M. Milgrom, M. B. Murataliev, and P. D. Boyer, *Biochem. J.* **330**, 1037 (1998).
- ³⁷R. K. Nakamoto, C. J. Ketchum, and M. K. Al-Shawi, *Annu. Rev. Biophys. Biomol. Struct.* **28**, 205 (1999).
- ³⁸J. Weber and A. E. Senior, *Biochim. Biophys. Acta* **1219**, 19 (1997).
- ³⁹S. Nadanaciva, J. Weber, and A. E. Senior, *J. Biochem. (Tokyo)* **39**, 9583 (2000).
- ⁴⁰J. Weber and A. E. Senior, *Biochim. Biophys. Acta* **1553**, 188 (2002).
- ⁴¹H. Y. Wang and G. Oster, *Europhys. Lett.* **57**, 134 (2002).
- ⁴²R. D. Astumian, *Science* **276**, 917 (1997).
- ⁴³C. Bustamante, D. Keller, and G. Oster, *Acc. Chem. Res.* **34**, 412 (2001); also, D. Keller and C. Bustamante, *Biophys. J.* **78**, 541 (2000).
- ⁴⁴S. Y. Sheu and D. Y. Yang, *J. Chem. Phys.* **114**, 3325 (2001).
- ⁴⁵S. P. Tsunoda, A. J. W. Rodgers, R. Aggeler, M. C. J. Wilce, M. Yoshida, and R. A. Capaldi, *Proc. Natl. Acad. Sci. U.S.A.* **98**, 6560 (2001).